EDM Proton R&D Plan for Simulation

F.Lin, A.U.Luccio, N.Malitsky

December 2, 2009

1 Status, Progress, Plan

1.1 Model Selection and Improvement

The original simulation environment was the combination of MAD[1] and SPINK[2] (MAD designs the ring lattice and generates the transport maps for all of elements, SPINK tracks the particle and spin motion based on the lattice and map information from MAD), which considered only partially nonlinear effect of the orbit on spin motion, like those generated by multipoles and magnet fringe effects. Besides, the second order maps generated by MAD proved not to be correct or complete, resulting in that the beam motion is unstable in a long term tracking. Thus, some nonlinear effects like the important quadratic term of the particle trajectory in calculating and correcting the spin coherence time have to be ignored. In addition, only first and second order maps were not adequate for our case because of unavoidable truncation problems. Higher order accurate maps are required to use SPINK as a spin tracker for the EDM.

The UAL[3] library allows one to generate these higher order transport maps since this environment allows to use as modules different developed object-oriented programs, such as PAC (Platform for Accelerator Codes), TEAPOT (Thin Element Program for Optics and Tracking), ZLIB (Numerical Library for Differential Algebra), etc. In UAL, these maps can be calculated with the ZLIB library for differential algebra using the automatic differentiation approach. According to this technique, maps of arbitrary orders are propagated through equations of motions in the same way as 6-dimensional vectors of coordinates. As a first step, the automatic differentiation procedure was implemented as a small script which generated the map coefficients and writes them into files loaded by the SPINK program. The maps information was compared with that produced by tother tools, e.g. PTC, thus giving us confidence in the correctness of he procedure.

SPINK, used as a stand-alone code and as a spin tracking module after the generation of transport maps by UAL, existed for a certain time period and several simulations have been carried out to investigate the spin coherence time. However, there was an important problem: the higher order maps coefficients for all elements had to be generated and stored in advance to be used by SPINK, which not only occupy a large space in computer memory, but also reduce the performance in the simulation. This is particularly bad with thin lens tracking (as is done in SPINK) where each machine element is cut to several slices to increase the accuracy of results. A better solution is to calculate the spin motion on the fly while tracking the particle trajectory in the storage ring. This was naturally implemented in UAL, when SPINK was treated like every other module in the library.

The spin module uses the basic SPINK algorithm by spin kicks for spin 1/2 polarized particles. The spin is treated as a 3-dimension real vector. The "accelerator" coordinate system is followed as a reference with x radial, y vertical and z longitudinal. The spin vector is transported through the accelerator by 3x3 matrices for thin elements. Spin matrices for thin elements are calculated from the Thomas-BMT equation:

$$\frac{d\mathbf{S}}{dt} = \frac{e}{m}\mathbf{S} \times \left[\left(a + \frac{1}{\gamma} \right) \mathbf{B} - a\frac{\gamma}{\gamma+1} \left(\vec{\beta} \cdot \mathbf{B} \right) \vec{\beta} - \left(\frac{g}{2} - \frac{\gamma}{\gamma+1} \right) \frac{\vec{\beta} \times \mathbf{E}}{c} \right], \tag{1}$$

where $a = (g-2)/2$ is the anomalous magnetic moment, $\mathbf{B}$ and $\mathbf{E}$ stand for the magnetic field and electric field, respectively. The propagation of the phase space coordinates of the beam through each

element is done in UAL. The local **B** and **E** field in the BMT equation are obtained from the beam transverse position in every lattice element, or each slice. For an instance, the three components of magnetic field in a dipole with field gradients

$$k_1 = \frac{\partial B_y/\partial x}{(B\rho)} \quad \text{and} \quad k_2 = \frac{\partial^2 B_y}{2(B\rho)}$$

are given by

$$\begin{cases} B_x = (B\rho)(k_1 y + 2k_2 xy) \\ B_y = (B\rho)\left(\frac{1}{\rho_0} + k_1 x - \frac{k_1 y^2}{2\rho_0} + k_2(x^2 - y^2)\right) \\ B_z = 0 \end{cases} . \tag{2}$$

The problem of field calculation in SPINK was corrected by giving a more precise definition of particle quadratic trajectory and dependent factors that were erroneously calculated using MAD generated second order maps. These errors were not relevant in early runs with SPINK for a large accelerator, like AGS and RHIC, but become important in machines like the EDM with small radii of curvature of the orbit.

In conclusion, the implementation of a spin module SPINK in the UAL gives us the right tool to propagate both the beam and spin, resulting that the impact of the electric dipole moment on the spin vector can be observed and analyzed with confidence for a very large number of turns and a large number of representative particles, in a comparatively short run time.

Another advantage of this scheme is that SPINK allows in a simple and direct way the calculation of spin coherence from the eigenvalue of the one-turn spin matrix. This method has been used for a study of the spin coherence of a beam of polarized deuterons in the storage ring COSY at Jülich[4]

1.2 Analytical and Numerical Studies on Simple Lattices

The strategy to study particle motion in UAL is to use the module TEAPOT for beam propagation in combination with the module SPINK for spin tracking; both modules using thin lens approximation for orbit and spin tracking, respectively. How thin each tracking slice should be is one of the issues to address for the accuracy of the results.

One way to test the accuracy of a simulation is to consider a specific problem of which we know the solution on theoretical grounds. A good example, as part of the calibration effort for the EDM experiment, is the study of the pitch effect[5], i.e. the correction on the (g-2) spin precession frequency of the spin motion of a circulating particle in a continuous ring with weak magnetic focusing, when the particle moves with a vertical oscillation.

The pitch corrected frequency $omega_a$ should be related to the uncorrected frequency ω_0 as follows (see Appendix I)

$$\omega_a = \omega_0 \left\{ 1 - \frac{1}{4}\left[1 - \frac{\omega_0^2 + 2a\gamma^2\omega_y^2}{\gamma^2(\omega_0^2 - \omega_y^2)} \right] \Psi_0^2 + \frac{n}{2(1-n)}\Psi_0^2 + \frac{1}{4}\Psi_0^2 \right\}, \tag{3}$$

when

- the magnetic field is weak focusing as

$$\begin{cases} B_x(x,y) = B_0\left[-\frac{n}{\rho_0} y + \frac{2b}{\rho_0^2} xy + ... \right] \\ B_y(x,y) = B_0\left[1 - \frac{n}{\rho_0} x + \frac{b}{\rho_0^2} - \frac{1}{2}\left(-\frac{n}{\rho_0^2} + \frac{2b}{\rho_0^2} \right) y^2 + ... \right] \\ B_z(x,y) = 0 \end{cases} ; \tag{4}$$

- The full momentum is constant, while the planar radius of the particle trajectory depends on the square of pitch angle.

Here Ψ_0 is the amplitude of the pitch angle, $\omega_0 = a(e/mc)B_y = a(e/mc)B_o$ is the (g-2) frequency for $\Psi_0 = 0$, ω_y is the frequency of the vertical oscillation, $n = -(\rho_0/B_0)(\partial B_y/\partial x)$ represents the focusing index, and $b = (\rho_0^2)/(2B_0)(\partial^2 B_y/\partial x^2)$ represents the sextupole component.

In the limit of fast pitch changes $\omega_y >> \omega_0$, it is

$$\omega_a = \omega_0 \left[1 - \frac{1+2a}{4}\Psi_0^2 + \frac{n}{2(1-n)}\Psi_0^2 + \frac{1}{4}\Psi_0^2\right] \tag{5}$$

Eq.(5) shows that the spin precession frequency ω_a has a quadratic dependence on pitch angle Ψ_0 for a given anomalous magnetic moment a and focusing index n. The simulation should be able to observe the modified spin precession frequency if the approximation is accurate enough.

A simple muon ring lattice with the parameters in Table 1 was employed for the testing.

Table 1

Muon momentum	$p = 0.1 GeV/c$
Weak focusing index	$n = 0.13$
Radius	$\rho = 5$ m
Anomalous magnetic moment	$a = 0.00116592$
Initial pitch angle	$\Psi_0 = 1$ mrad
Initial spin vector	$(S_x, S_y, S_z) = 0, 0, 1$

With only weak focusing index, the magnetic field is given as

$$\begin{cases} B_x(x,y) = B_0\left(-\dfrac{n}{\rho_0}y\right) \\ B_y(x,y) = B_0\left(1 - \dfrac{n}{\rho_0}x + \dfrac{n}{2\rho_0^2}y^2\right) \\ B_z = 0 \end{cases} \tag{6}$$

The averaged radius shift is obtained as[**?**][10]

$$< \Delta\rho > \approx \frac{\rho}{1-n}\left[\left(\frac{\Delta p}{p}\right)_{pl} - \frac{n}{2\rho^2} < y^2 >\right] = -\frac{\rho}{1-n}\frac{\Psi_0^2}{2}. \tag{7}$$

Therefore, the averaged radius shift and the correction of (g-2) frequency are two criterions for checking the simulation environment form both particle and spin motion point of view. For the above muon ring lattice, n equals 0.13, resulting in $\omega_y/\omega_0 \approx 225$, close to the limit of fast pitch change. Given the initial pitch angle $\Psi_0 =$ mrad, the averaged radius shift is -2.87×10^{-6} m (- sign means the radius shifts inside of the designed orbit) and the ratio $(\omega_a - \omega_0)/\omega_0 \approx 7.42 \times 10^{-8}$. A reliable simulation should be able to reproduce these results.

In order to show these results conveniently, Figs.1 and 2 only plot the particle orbit motions in the first 1-100 turn and the last 9900-10000 turn from the tracking of UAL and COSY-INFINITY[6]. These two trackings agree to each other very well, and the averaged radius shifts around -2.87×10^{-6} m also have a very similar value with that from the above formula. Fig.3 plots the spin (g-2) precession ($\vec{\nu}\cdot\mathbf{S}$) vs. turn in the first 1000 turn from UAL and COSY-INFINITY. Similarly to the agreement in particle motion, the results from the two simulation tools also agree well.

Using the same procedure, the calculated ratios $(\omega_a - \omega_0)/\omega_0$ are listed in Table 2. Within the uncertainty, both of the two results agree with the analytical value $(\omega_a - \omega_0)/\omega_0 = 7.42 \times 10^{-8}$.

In a different approach we have used the differential equations from J.D.Jackson[11] shown here in rationalized MKS units

$$\frac{d\vec{\beta}}{dt} = \frac{e}{m\gamma}\left[\frac{\mathbf{E}}{c} + \vec{\beta}\times\mathbf{B} - \frac{(\vec{\beta}\cdot\mathbf{E})\vec{\beta}}{c}\right] \tag{8}$$

and

$$\frac{d\mathbf{S}}{dt} = \frac{e}{m}\mathbf{S}\times\left[\left(a+\frac{1}{\gamma}\right)\mathbf{B} - \frac{a\gamma}{\gamma+1}(\vec{\beta}\cdot\mathbf{B})\vec{\beta} + \left(a+\frac{1}{\gamma+1}\right)\frac{\vec{\beta}\times\mathbf{E}}{c}\right] \tag{9}$$

The integration of the above equations was done numerically using the subroutine DHPCG[7] based on a fourth order predictor-corrector algorithm with Runge-Kutta as a starter and automatic halving of the integration step. The initial time step used was 0.5ps and on a 2.5 GHz Xeon CPU it takes about 102 s to track a single particle in the ring for 30μs. This method is obviously very slow but at the same time it is also very simple and accurate. The pitch correction, for the same situation of muon in that weak focusing ring is found to be $(7.6 \pm 0.2) \times 10^{-8}$ as shown in Table 2. Also the horizontal and vertical motions from this approach are shown in Figs.**??** and 5, which similarly present the averaged radius shifts around -2.85×10^{-8} m.

Tool	$\frac{\omega_a - \omega_0}{\omega_0} \times 10^{-8}$
UAL	7.38 ± -0.03
COSY-Infinity	7.40 ± -0.02
DHPCG	7.6 ± -0.2

Table 2. Calculated ratios of from UAL, COSY-INFINITY and DHPCG Integration.

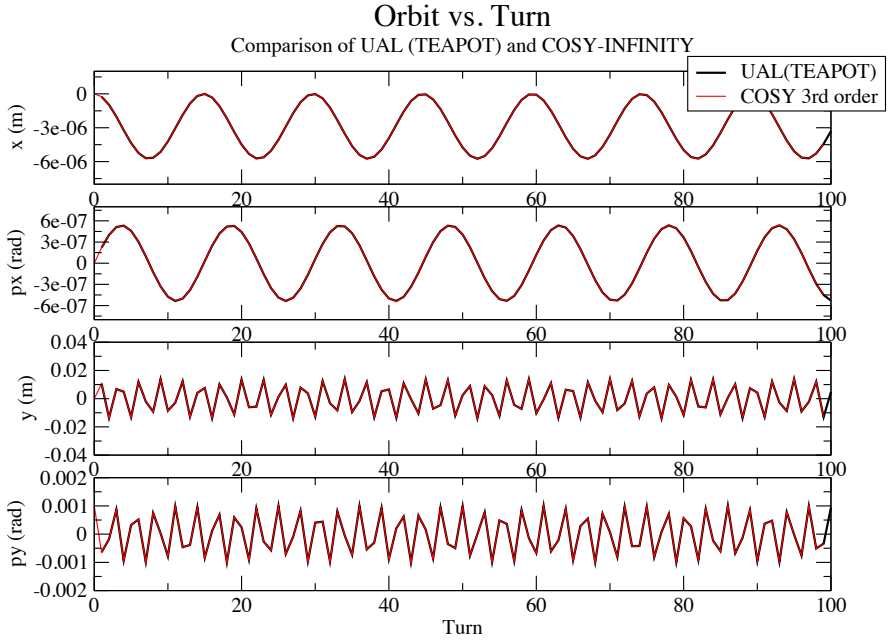

Figure 1: Particle radital and vertical motioon in the first 1-100 turn from UAL and COSY-Infinity. The average radius shifts are both around 2.85×10^{-6}

In conclusion, using the weakly focusing magnetic field ring lattice, the tracking results (the shifted averaged radius and corrected (g-2) spin precession frequency) from UAL with SPINK module agree with that from the analytical calculation, COSY-INFINITY and the Integration of differential equations.

However, UAL has more flexibility for developing new extensions, such as new types of elements and enhancing the accuracy of the original approach with the slicing technique, which is paramount in the EDM experiment due to the requirement of the radial electric field in the vertical magnetic field range or pure radial electric field instead of vertical magnetic field. The introduced radial E field not only affects the horizontal motion, but also causes the energy variation that is normally not treated in most of accelerator simulation tools, like the original TEAPOT.

Since UAL uses a TEAPOT module for particle beam motion tracking, the extension of particle motion due to the electric field has to be added externally. This implement is performed following

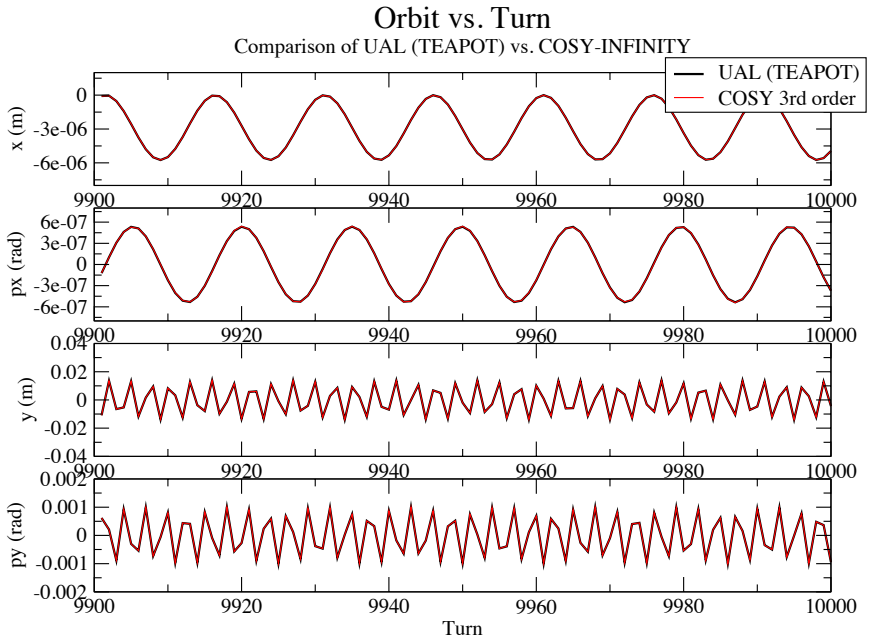

Figure 2: Particle radial and vertical motion in the last 9900-10000 turns from UAL and COSY-Infinity. The average radius shifts are both around 2.85×10^{-6}

the Lorentz equations described in the Frénet-Serret coordinate system

$$\begin{cases} \dfrac{d}{ds}\left(\dfrac{p_x}{p_0}\right) = \dfrac{e}{p_0 c}\left[\dfrac{\mathbf{E}}{\beta_0} + \dfrac{\mathbf{p}}{p_0} \times \mathbf{B}\right]_x \left(\dfrac{dt}{ds} v_0\right) + h\dfrac{p_z}{p_0} \\ \dfrac{d}{ds}\left(\dfrac{p_y}{p_0}\right) = \dfrac{e}{p_0 c}\left[\dfrac{\mathbf{E}}{\beta_0} + \dfrac{\mathbf{p}}{p_0} \times \mathbf{B}\right]_y \left(\dfrac{dt}{ds} v_0\right) \\ \dfrac{d}{ds}\left(\dfrac{\epsilon}{p_0}\right) = \dfrac{e\mathbf{E}}{p_0 c} \cdot \dfrac{\mathbf{p}}{p_0}\left(\dfrac{dt}{ds} v_0\right) \end{cases} . \tag{10}$$

with

$$\frac{dt}{ds} = \frac{1 + hx}{p_z/p_0}\frac{1}{v_0}, \qquad \frac{p_z}{p_0} = \sqrt{\frac{\epsilon^2 - (m_0 c^2)^2}{(p_0 c)^2} - \frac{p_x^2 + p_y^2}{p_0^2}}$$

The implementation of this part presents some new problems for the simulation by thin element kicks by TEAPOT, since the energy of the particle receives a sudden kick that is calculated at the kick location (*e.g.* x in the factor $1 + hx$ in the preceding equations). Figs.6 and **??** show the evolution of the radial profile and of the energy of the beam after hundreds of turns, for a series of thinner and thinner of the same element (electrostatic dipoles in a model ring). The result is that in the long run the energy of the particle, hence the amplitude of the oscillations, shows a disturbing and unphysical growth. The problem is being solved by introducing in the expressions some smart extrapolated values of the quantity x between the kick and the next kick. It is interesting to observe that a similar problem doesn't appear for magnetic kicks, that do not affect the energy of the particle.

1.3 Experimental Studies at Existing Facilities (*e.g.* COSY)

The polarized proton and deuteron synchrotron COSY at the KFZ laboratory at Jülich, Germany, is a very useful reference facility to perform low energy polarized beams experiments for the EDM.

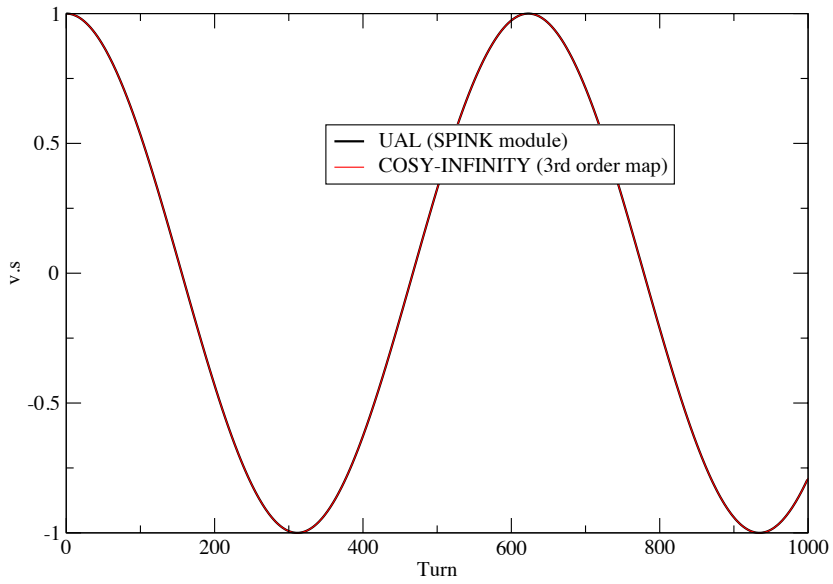

Figure 3: Spin (g-2) precession ($\mathbf{v} \cdot \mathbf{S}$)

There is an already established and ongoing collaboration on the subject.

Among others, two main areas of research at COSY of interest for the EDM are:

1. Experimental studies of spin coherence time and methods to make it as long as possible, in particular with the use of sextupoles (available at COSY for chromaticity correction). A first numerical SPINK simulation study on the problem has just been completed[4].

2. Experimental studies of methods to flip the polarization of spin 1/2 particles from vertical to longitudinal using RF solenoids (available at COSY) or other devices. SPINK simulation studies of the RF devices at COSY have been already performed and results published[8]. Another SPINK tracking study, specifically aimed at the EDM issues, is in progress.

1.4 Appendix I

In most accelerator physics manuals, the components of the magnetic field are expanded in terms of dipole (constant), quadrupole (first order), sextupole (second order), etc[1]. Independent of time and to second order, for a circular machine the expansions of the magnetic field components can be expressed in the form

$$\begin{cases} B_x(x,y) = B_0 \left[-n\dfrac{y}{\rho_0} + 2b\dfrac{xy}{\rho_0^2} + ... \right] \\ B_y(x,y) = B_0 \left[\dfrac{x}{\rho_0}x + b\dfrac{x^2}{\rho_0^2} - \dfrac{1}{2}\left(-(n-2b)\dfrac{y^2}{\rho_0^2} \right) + ... \right] \\ B_z(x,y) = 0 \end{cases} .$$

Here (x, y, z) represent the directions of radially outward, vertically up and longitudinally forward respectively. ρ_0 is the radius of the ring. B_0 is the constant dipole magnetic field at $x = y = 0$.
$n = -(\rho_0/B_0)(\partial B_y/\partial x)$ is the field focusing index and represents the quadrupole component.
$b = (\rho_0^2/2B_0)(\partial^2 B_y/\partial x^2)$ represents the sextupole component.

Let us assume a continuous ring made by a single 360^0 bending magnet:

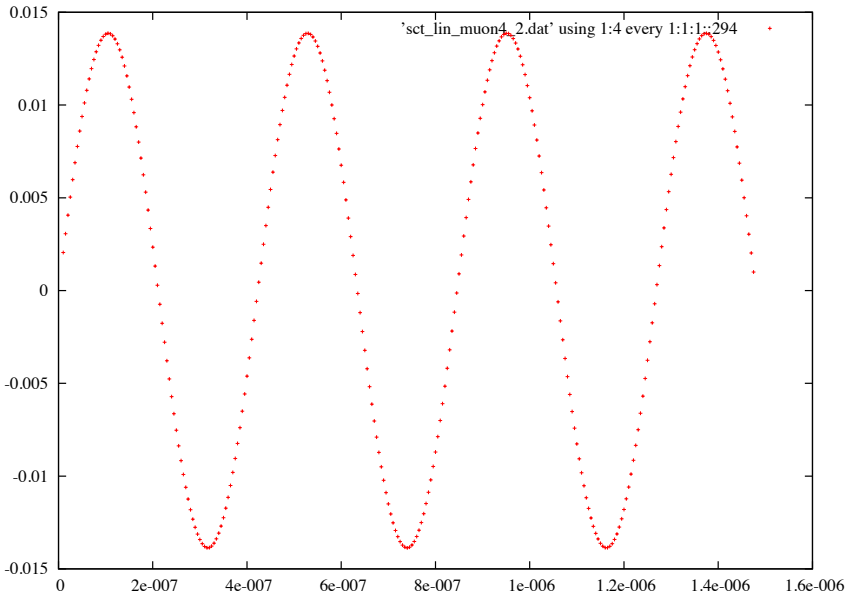

Figure 4: Vertical motion vs. time from the integration of differential equations.

1. when both $n = 0$ and $b = 0$, a uniform magnetic field without any focusing is given as

$$\begin{cases} B_x(x,y) = 0 \\ B_y(x,y) = B_0 \\ B_z = 0 \end{cases} ;$$

2. when $n \neq 0$ and $b = 0$, a magnetic field with a quadrupole component (weak focusing) is given as

$$\begin{cases} B_x(x,y) = B_0 \left(-n \dfrac{y}{\rho_0} \right) \\ B_y(x,y) = B_0 \left(-n \dfrac{x}{\rho_0} + n \dfrac{y^2}{2\rho_0^2} \right) \\ B_z(x,y) = 0 \end{cases} ;$$

3. when $n/neq0$ and $b/neq0$, a magnetic field with both quadrupole and sextupole component, B_y in the previous equation can be rewritten as

$$B_y(x,y) = B_0 \left[1 - n \frac{x}{\rho_0} + n \frac{y^2}{2\rho^2} + b \frac{x^2 - y^2}{\rho_0^2} \right].$$

Those additional first and second order terms in the magnetic field cause a significant pitch correction in the (g-2) spin precession frequency.

Consider a simple ring composed of homogeneously distributed magnetic fields with the most general condition of $n \neq 0$ and $b \neq 0$. Assume a particle is circulating in such a ring at an initial small vertical angle Ψ_0 (pitch angle) with respect to the (xy) plane, perpendicular to the $\hat{y}$ axis. The pitch angle varies harmonically due to the vertical focusing force (radial components of magnetic field) as

$$\Psi = \Psi_0 \cos \omega_y t,$$

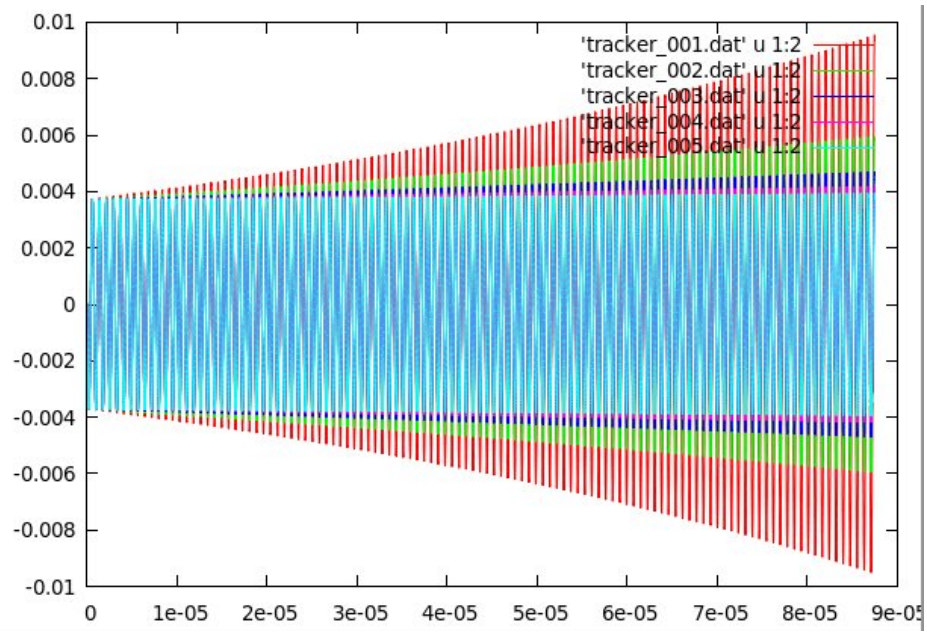

Figure 5: Radial profile of a particle in the beam acted upon by electrostatic bending dipoles after subdivision in 4, 8, 16, 32 and 64 slices.

with ω_y the frequency of the vertical oscillation. The vertical motion of the particle is given by $y = y_0 \sin \omega_y t$. Keeping the same momentum of the particle with the initial pitch angle, the planar projection of the momentum $p_{pl} = p \cos \Psi$ causes the radius of the trajectory to shift as $\rho_{pl} = \rho_0 \cos \Psi$.

Because of the horizontal focusing force, the particle experiences an oscillation in the horizontal plane. The horizontal motion with respect to the reference orbit includes two terms:

$$x =< \Delta\rho > + x_0 \cos \omega_x t, \qquad x_\beta = x_0 \cos \omega_x t.$$

$< \Delta\rho >$ is the radius shift with respect to the designed value, and x_β is the horizontal oscillation amplitude around the equilibrium orbit. Here is the average shift of the radius. ω_x is the horizontal oscillation frequency.

In the rotating frame about the $\hat{y}$ axis at frequency $\omega_r = (e/mc\gamma)B_y$[10], the spin frequency is

$$\omega_a = a\frac{e}{mc\gamma}B^*,$$

where $a = (g-2)/2$ and B^* is the magnetic field in the rest frame of the particle. In such rotating frame, the frequency of spin precession is called the (g-2) frequency. The vertical component B_y of the magnetic field is not constant if the particle has a radial (x) and vertical (y) motion ($B_y = B_0$ if the pitch angle equals zero). As shown before, both radial and vertical motion contribute to the correction of the vertical magnetic field B_y seen by a particle. By time average, the linear term x_β is zero. The average radius change $< \Delta\rho >$ and the quadratic nonlinearity of $n(y^2/2\rho 2)$ and $b(x^2 - y^2)(\rho^2$ due to the vertical motion contribute to the vertical magnetic field B_y.

For a uniform continuous magnetic field ring, the vertical component of ω_a is

$$\omega_{ay} = \omega_0 \left(1 - \frac{\gamma - 1}{\gamma}\Psi^2\right),$$

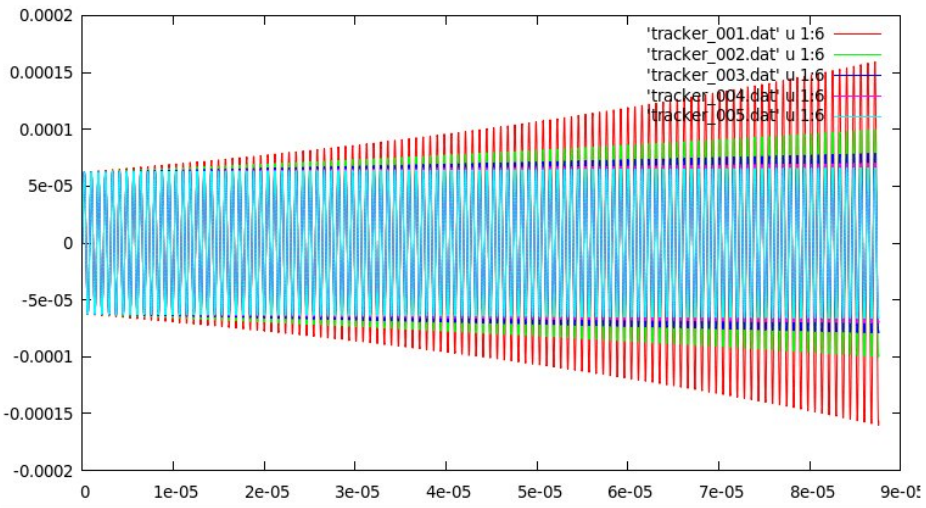

Figure 6: Energy profile of a particle in the beam acted upon by electrostatic bending dipoles after subdivision in 4, 8, 16, 32 and 64 slices.

where $\omega_0 = a(e/mc)B_y = a(e/mc)B_0$ is the (g-2) frequency for $\Psi = 0$. Therefore, the observed (g-2) frequency is

$$\omega_a = \omega_0(1-C), \quad \text{with the correction factor[9]} \quad C = \frac{1}{4}\Psi_0^2\left[1 - \frac{\omega_0^2 + 2a\gamma^2\omega_y^2}{\gamma^2(\omega_0^2 - \omega_y^2)}\right].$$

When $\omega_y >> \omega_0$, C is approaching the value $\Psi_0^2[1+2a]/4$.

For a more general ring case, the radius shift and the quadratic nonlinear term significantly revise the vertical magnetic field as previously given, resulting in the expression of ω_0 as

$$\omega_{0,new} = a\frac{e}{mc} < B_y >= a\frac{e}{mc}B_0(1+D),$$

with the correction factor

$$D = -n\frac{< x >}{\rho} + n\frac{< y^2 >}{2\rho^2} + b\frac{< x^2 > - < y^2 >}{\rho^2}.$$

Correspondingly, the observed (g-2) frequency ω_a is obtained

$$\omega_a = \omega_0\left[1 - \frac{1}{4}\left(1 - \frac{\omega_0^2 + 2a\gamma^2\omega_y^2}{\gamma^2(\omega_0^2 - \omega_y^2)}\right) - n\left(\frac{< \Delta\rho >}{\rho} - \frac{y_0^2}{4\rho^2}\right) + b\frac{< \Delta\rho >^2 + x_0^2/2 - y_0^2/2}{\rho^2}\right]$$

where higher order corrections are negligible. An immediate conclusion is obtained that the correction to the observed (g-2) spin precession frequency can be zero if the values of n and b are properly chosen.

Let us consider one case that only weak focusing is included (quadrupole effect $n \neq 0$, but sextupole effect $b = 0$), two relevant relations are obtained[9]

$$< \Delta\rho > \approx -\frac{\Psi_0^2}{2(i-n)}\rho, \quad y_0\frac{\Psi_0}{\sqrt{n}}\rho.$$

In this case, ω_a is rewritten as

$$\omega_a = \omega_0\left[1 - \frac{1}{4}\left(1 - \frac{\omega_0^2 + 2a\gamma^2\omega_y^2}{\gamma^2(\omega_0^2 - \omega_y^2)}\right) - \frac{n}{2(1-n)}\Psi_0^2 + \frac{1}{4}\Psi_0^2\right].$$

For a given particle with a non zero pitch angle, the quadrupole (n) and sextupole (b) components give additional correction to the observed (g-2) spin frequency, which can be slower or faster (even equal) to that of particle without pitch angle. This results in an important conclusion that the spin frequency can be tuned on request by the focusing index n, for example the quadratic correction to the frozen spin precession in the deuteron electric dipole moment experiment[12].

The limit of slow pitch rate of changes ($\omega_y << \omega_0$)

$$\omega_a \approx \omega_0 \left[1 - \frac{\beta^2}{4}\Psi_0^2 + \frac{n}{2(1-n)}\Psi_0^2 + \frac{1}{4}\Psi_0^2\right].$$

When ω_y increases and arrives to the limit of fast pitch changes ($\omega_y >> \omega_0$), it is

$$\omega_a \approx \omega_0 \left[1 - \frac{1+2a}{4}\Psi_0^2 + \frac{n}{2(1-n)}\Psi_0^2 + \frac{1}{4}\Psi_0^2\right].$$

References

[1] *MAD Program, Physical Methods Manual*

[2] A.U.Luccio, *Project: SPINK*, Proc SPIN2008, Charlottesville, VA

[3] N.Malitsky and R.Talman, *Unified Accelerator Libraries*. AIP 391 http://code.google.com/p/ual (1996)

[4] A.U.Luccio, F.Lin, C.J.G. Onderwater and E.J.Stephenson, *Tracking studies of spin coherence in COSY in view of EDM polarization measurements*, Proc. PST2009, Ferrara, Italy, September 7-11 (2009)

[5] F.J.M.Farley, *Pitch Correction in (g-2) Experiments*, Physics Letter Vol. 42B, No.1, p.66 (1972)

[6] COSY-INFINITY version 9.0, (C) MSU 1995-2009

[7] DHPCG, solver of a system of differential equations using a fourth order predictor-corrector algorithm, from the scientific subroutine package (SSP) by IBM.

[8] A.U.Luccio and A.Lehrach, Proc. EPAC08, Genova, Italy (2008)

[9] Y.F.Orlov, *All Simulations of the Azimuthally Homogeneous Ring are Correct (so far)*, EDM note August 2 (2008)

[10] Y.F.Orlov, *Spin Coherence Time (SCT) I-IV: Using Normal Co-ordinates in the Analysis of SCT*, EDM note June (2008)

[11] J.D.Jackson, *Classical Electrodynamics*, p.559, 2nd Ed., (1975)

[12] *Search for a permanent electric dipole moment of the deuteron nucleus at the 10-29 e.cm level*, AGS proposal (2008)